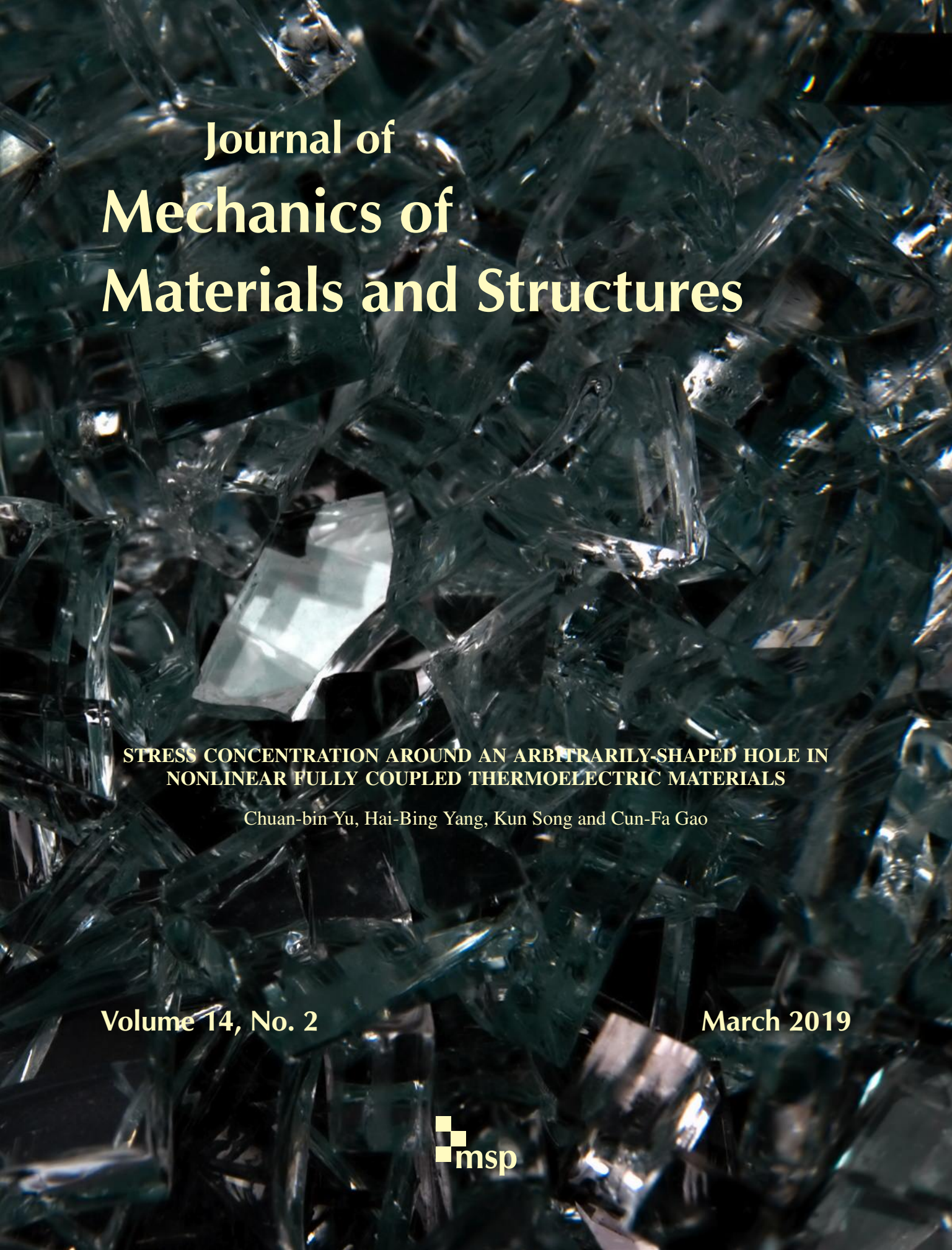

Journal of
Mechanics of
Materials and Structures

STRESS CONCENTRATION AROUND AN ARBITRARILY-SHAPED HOLE IN NONLINEAR FULLY COUPLED THERMOELECTRIC MATERIALS

Chuan-bin Yu, Hai-Bing Yang, Kun Song and Cun-Fa Gao

Volume 14, No. 2 March 2019

msp

JOURNAL OF MECHANICS OF MATERIALS AND STRUCTURES
Vol. 14, No. 2, 2019
dx.doi.org/10.2140/jomms.2019.14.259

STRESS CONCENTRATION AROUND AN ARBITRARILY-SHAPED HOLE IN NONLINEAR FULLY COUPLED THERMOELECTRIC MATERIALS

CHUAN-BIN YU, HAI-BING YANG, KUN SONG AND CUN-FA GAO

Using the complex variable method, we study the plane problem of an infinite thermoelectric material containing an arbitrarily-shaped hole under a uniform remote electric current and a uniform energy flux. The nonlinear fully coupled thermoelectric constitutive equations are used to account for the large current or temperature gradient imposed on thermoelectric materials during their engineering service. The hole surface is assumed to be electrically and thermally insulated and mechanically free. The shape of the hole is defined by a polynomial conformal mapping. Fourier expansion technique is used to solve the corresponding boundary value problems. A triangular hole is considered for the purpose of illustration. The bluntness, hole orientation and the load angle as important parameters are considered. Numerical results show that the effects of these parameters on stress distribution around the hole are very significant. By the correct selection of these parameters, the lowest thermal stress concentration can be achieved.

1. Introduction

Thermoelectric materials are widely used in energy conversion: the Seebeck effect allows electricity generation from a temperature gradient, while the Peltier effect can convert electricity into cooling [Tritt and Subramanian 2006; Bell 2008; He et al. 2015; He and Tritt 2017]. Thermoelectric solids are typically brittle semiconductors with low mechanical strength and always subjected to defects and damages, for example, holes, voids and cracks, during their fabrication and operation [Schmidt et al. 2015; Li et al. 2015]. When the heat flux at a thermoelectric solid is disturbed by the geometric discontinuities brought by holes/imperfections, thermal stresses are induced. Excessive thermal stresses will cause the premature failure and thus reduce the useful life of thermoelectric structures and devices. Determining the amount and location of these stresses is essential to achieve accurate predict and evaluate the reliability of thermoelectric devices. Consequently, the research on the hole problem of thermoelectric materials is of great practical importance.

Thermal stress concentration around holes is one of the classical topics in solid mechanics. Ever since Florence and Goodier [1960] developed the basic theory of thermoelasticity in which complex variable method for stress analysis of perforated plate was used, the research on thermal stress concentration problem around holes is ongoing. For instance, using the complex variable theory, Chao and Wang [1993] predicted the failure initiation and crack trajectory for a plate weakened by an elliptic hole under thermal or mechanical load based on the strain energy density criterion. The Green's function for an infinite isotropic plate with an arbitrary-shaped hole under adiabatic and isothermal boundary conditions with a heat source was obtained by Yoshikawa and Hasebe [1999]. Based on Green's function method and the technique of conformal mapping, a unified solution for a thermopiezoelectric plate with holes

Keywords: thermoelectric materials, conformal mapping, series expansion, arbitrarily-shaped holes, thermal stress.

of various shapes was obtained analytically by Qin [1999; 2000]. Based on the extended version of Eshelby–Stroh's formulation, Gao et al. [2002] studied the generalized plane problem of an elliptical hole in a thermopiezoelectric medium subjected to uniform heat flow and mechanical-electrical loads at infinity according to exact boundary conditions at the rim of the hole. The two-dimensional thermoelastic problems for the perforated plates for different mechanical and thermal boundary conditions were fully investigated by Hasebe and Wang [2005]. The general solutions for the external force, displacement, and mixed boundary value problems under both the uniform heat flux and a point heat source were separately described. Thermoelastic solution to a coated elliptic hole embedded in an infinite plate under uniform heat flux was investigated by Chen and Chao [2008]. Hasebe and his coworkers analyzed the Joule heat, temperature and thermal stress induced by an electric current for a thin infinite conductor containing an elliptical hole, and the similar stress analysis was extended for magnetoelastic materials [Hasebe et al. 2009; Hasebe 2009]. With using the method of piece-wise homogeneous layers, the non-axisymmetric two-dimensional problem of thermal stresses in a functionally graded plate having radial arbitrary elastic properties with a circular hole under remote uniform heat flux is derived by Yang and Gao [2010]. Lekhnitskii's complex variable method was developed by Rasouli and Jafari to investigate the effect of uniform heat flux on a perforated anisotropic plate with an elliptical hole [Rasouli and Jafari 2016]. Additionally, Jafari et al. [2016] studied the effect of rotation angle and bluntness of hole on stress distribution around an arbitrary-shaped hole in an infinite isotropic plate based on the complex variable method and conformal mapping technique.

Many of the work done by the various researchers highlight the importance of thermal stress analysis around holes in thermoelasticity governing by linear equations. However, coupling among different physical phenomena makes the analysis in nonlinear media considerably more complicated. One such example is thermoelectricity, wherein the electric and heat transports are nonlinearly coupled. Up to present, the investigations on the hole problem in thermoelectric materials are restricted to holes with regular shape (circular and elliptical hole) due to the complicated nonlinear governing equations. For examples, Zhang and Wang investigated the elliptical hole problem in an infinite thermoelectric medium when electric current and energy flux loads are perpendicular to the major axis of the elliptical hole [Zhang and Wang 2016]. The plane problem of an inclined elliptic hole in an infinite thermoelectric material was studied by Wang and Wang [2017]. Pang et al. [2018] analyzed the temperature, heat flux and thermal stress induced by an electric current for a thin infinite thermoelectric medium containing a circular hole with an edge crack. To the best of our knowledge, no study has been completely conducted to evaluate the thermal stresses in a thermoelectric material containing a hole with irregular shapes. In fact, holes/imperfections of different shapes are made up due to practical reasons. Stresses concentration will occur at the contour of the hole and its analysis involves lot of complexity. In the present study, by using the complex variable method and conformal mapping technique [Muskhelishvili 1975], an attempt has been made to show the influence of key parameters such as rotation angle and bluntness on the thermal stress distribution around practical holes with various shapes.

2. Basic equations for thermoelectric materials

2.1. ***Governing quations.*** We consider a homogeneous and isotropic thermoelectric medium characterized by the electric conductivity δ, thermal conductivity κ and Seebeck coefficient ε. The constitutive

euqations governing the coupled transports of heat and electricity in such a material can be given by [Zhang and Wang 2016; Yang et al. 2013]

$$\boldsymbol{J} = -\delta\nabla\phi - \delta\varepsilon\nabla T = -\delta\nabla(\phi + \varepsilon T), \tag{1}$$

$$\boldsymbol{J}_q = -T\varepsilon\delta\nabla\phi - (T\varepsilon^2\delta + \kappa)\nabla T = \varepsilon T\boldsymbol{J} - \kappa\nabla T, \tag{2}$$

where ∇ is the Nabla operator, ϕ is the electric potential, T is the temperature, $\boldsymbol{J}$ and $\boldsymbol{J}_q$ are the electric current density vector and the thermal flux vector, respectively. Additionally, the thermoelectric equilibrium equations are expressed by

$$\nabla\cdot\boldsymbol{J} = 0, \qquad \nabla\cdot\boldsymbol{J}_u = 0, \tag{3}$$

where $\boldsymbol{J}_u$ is the energy flux vector defined as

$$\boldsymbol{J}_u = \boldsymbol{J}_q + \phi\boldsymbol{J}, \tag{4}$$

which indicates that the energy in the medium is transported by both electricity and heat. It is worth pointing out that the physical meaning of (3) is that both electric charges and energy are conserved in the considered material.

Obviously, the thermoelectric equations are nonlinear with fully coupled electric current and temperature. From (1), one can see that the Seebeck effect, which generates electric potential difference from temperature difference, will also produces electric current in the material. On the other hand, the electric current can cause extra heat flow in thermoelectric material in addition to the temperature gradient. The ratio of the generated extra heat flux to electric current is related to an intrinsic material property called Peltier coefficient $\Pi = \varepsilon T$. The uncoupled heat transfer and electric conduction problem, which renders the Fourier's law and Ohm's law, respectively, can be revealed by letting $\varepsilon = 0$. Introduce the thermoelectric potential function according to $H = \phi + \varepsilon T$ into (1)–(4), the thermoelectric constitutive and equilibrium equations can be rewritten as

$$\boldsymbol{J} = -\delta\nabla H, \qquad \boldsymbol{J}_u = H\boldsymbol{J} - \kappa\nabla T, \tag{5}$$

$$\nabla^2 H = 0, \qquad \kappa\nabla^2 T + \delta(\nabla H)^2 = 0. \tag{6}$$

The nonlinearity of the second in (6) makes the analysis in thermoelectric materials much more difficult. This will be illustrated below.

2.2. ***General solutions of thermoelectric field.*** Consider the generalized plane problem, in which all the physical quantities are assumed to be dependent on the in-plane coordinates (x, y). Note that the first in (6) is a Laplace's equation, the general solution then can be given by [Muskhelishvili 1975]

$$H = \operatorname{Re} f'(z), \tag{7}$$

where $f'(z)$ stands for an unknown potential function of complex variable $z = x + iy$ with i representing the imaginary unit and "Re" denoting the real part of a complex number. Combining (7) with the first in (5) gives

$$J_x - iJ_y = -\delta f''(z). \tag{8}$$

On the other hand, inserting (7) into the second of (6) gives rise to

$$\nabla^2 T = -\frac{\delta}{T}\{\nabla \operatorname{Re} f'(z)\}^2 = -\frac{\delta}{\kappa} f''(z)\,\overline{f''(z)}, \tag{9}$$

where the superimposed bar denotes the complex conjugate. Solution of (9) then can be expressed by the superposition of a particular solution and the homogenous solution as

$$T = -\frac{\delta}{4\kappa} f'(z)\,\overline{f'(z)} + \operatorname{Re} g'(z), \tag{10}$$

where $g'(z)$ is an analytic complex function. Making use of (7), (8) and (10), the energy flux can be obtained from the second in (5) as

$$J_{ux} - i\,J_{uy} = -\frac{\delta}{2} f''(z)\; f'(z) - \kappa g''(z). \tag{11}$$

The thermal flux components and electric potential can be obtained, respectively, from (2) and the identity $\phi = H - \varepsilon T$ together with (7), (8), (10) and (11). Since they will not be used directly in the analysis, they are not given in detail. The resultant electric current density and energy flux from any point P_1 to P_2 on a directed curve denoted by s can be derived from (8) and (11) as

$$\int_{P_1}^{P_2} J_n(s)\,ds = -\operatorname{Im}\,\delta f'(z)\Big|_{P_1}^{P_2}, \tag{12}$$

$$\int_{P_1}^{P_2} J_{un}(s)\,ds = -\operatorname{Im}\Big[\frac{\delta}{4} f'^2(z) + \kappa g'(z)\Big]\Big|_{P_1}^{P_2}, \tag{13}$$

where the subscript "n" represents the normal component and "Im" stands for the imaginary part of a complex number.

In this section, the mathematical formulation of the coupled electric and heat conduction problem is thus completed. Once the two analytic complex functions $f'(z)$ and $g'(z)$ are obtained from exact electric and thermal boundary conditions, then all the quantities associated with the electric and temperature field can be determined.

2.3. ***General solutions of stress field.*** In case the temperature on the thermoelectric plane (x, y) is obtained, the thermal stresses caused by the uneven temperature distribution can be determined according to the Hooke's law of thermoelasticity. By combining the equilibrium equations, compatibility equations, thermoelastic stress-strain relationship, one can easily obtain the governing equations in terms of Airy stress function U as [Hasebe et al. 2009; Wang and Wang 2017]

$$\nabla^4 U + E\lambda\nabla^2 T = 0, \tag{14}$$

where

$$E = \begin{cases} E_0, \\ E_0/(1-\nu_0^2), \end{cases} \qquad \lambda = \begin{cases} \lambda_0, & \text{plane stress}, \\ (1+\nu_0)\lambda_0, & \text{plane strain}, \end{cases}$$

where E_0, ν_0 and λ_0 are the Young's modulus, Poisson's ratio and thermal expansion coefficient.

Inserting (9) into (14) yields

$$\nabla^4 U = \frac{k\delta}{\kappa} f''(z)\,\overline{f''(z)}\,,$$

where $k = E_0\lambda_0$ for plane stress and $k = E_0\lambda_0/(1-\nu_0)$ for plane strain. The complete solution of U includes a particular solution and a homogeneous solution. Using superposition principle, stresses and displacement can be expressed in terms of $f(z)$ and $g(z)$ together with other two complex potentials $\varphi(z)$ and $\psi(z)$. Omitting details, the components of stresses and displacement can be given as [Wang and Wang 2017; Yu et al. 2017]

$$\begin{aligned} \sigma_{yy}+\sigma_{xx} &= \frac{k\delta}{4\kappa}\, f'(z)\,\overline{f'(z)} + 2[\varphi'(z)+\overline{\varphi'(z)}], \\ \sigma_{yy}-\sigma_{xx}+2i\sigma_{xy} &= \frac{k\delta}{4\kappa}\, f''(z)\,\overline{f(z)} + 2[\bar{z}\,\varphi''(z)+\psi'(z)], \end{aligned} \tag{15}$$

$$2\mu(u_x+iu_y) = \beta\,\varphi(z) - z\,\overline{\varphi'(z)} - \overline{\psi(z)} - \frac{k\delta}{8\kappa}\,\overline{f'(z)}\,f(z) + 2\mu\lambda\, g(z), \tag{16}$$

where μ is the shear modulus and

$$\beta = \begin{cases} \dfrac{3-\nu_0}{1+\nu_0} & \text{(plane stress)}, \\ 3-4\nu_0 & \text{(plane strain)}. \end{cases}$$

Additionally, the resultant forces (F_x, F_y) on a certain directed curve s from any point P_1 to P_2 can be expressed by [Wang and Wang 2017; Yu et al. 2017]

$$i\int_{P_1}^{P_2} (F_x + iF_y)\, ds = \Big[\varphi(z) + z\,\overline{\varphi'(z)} + \overline{\psi(z)} + \frac{k\delta}{8\kappa}\,\overline{f'(z)}\,f(z)\Big]\Big|_{P_1}^{P_2}. \tag{17}$$

The mathematical formulation of the plane thermoelastic problem in a thermoelectric material is presented next. Once the thermoelectric fields are obtained, the associated thermal stress field can be solved by determining the two complex potentials $\varphi(z)$ and $\psi(z)$ with the aid of elastic boundary conditions given in (16) and (17).

3. Thermoelectric plane with an arbitrarily-shaped hole

3.1. ***Problem description and boundary condition.*** As shown in Figure 1, we consider an infinite thermoelectric material containing a hole of practically arbitrary shape subjected to a uniform electric current density J^∞ and a uniform energy flux J_u^∞ at infinity, in an arbitrary direction γ with respect to the x-axis. It is assumed that no far-field mechanical loads are imposed and the medium can expand freely at infinity. Furthermore, the hole can take arbitrary orientation such that the major axis of the hole is directed at angle η with respect to horizontal axis. The hole surface is assumed to be electrically impermeable, thermally insulated and mechanically free. These conditions can be expressed by

$$\left.\begin{aligned} J_n &= 0 \\ J_{qn} = J_{un} &= 0 \\ \sigma_{nn}+i\sigma_{nt} &= 0 \end{aligned}\right\} \quad \text{on } L. \tag{18}$$

It should be mentioned that the thermally insulated boundary condition $J_{qn}=0$ is equivalent to $J_{un}=0$ according to (4) and the first of (18). In what follows, we solve the complex functions $f(z)$ and $g(z)$ to determine the electric field and temperature field using the first and second conditions given in (18). Then,

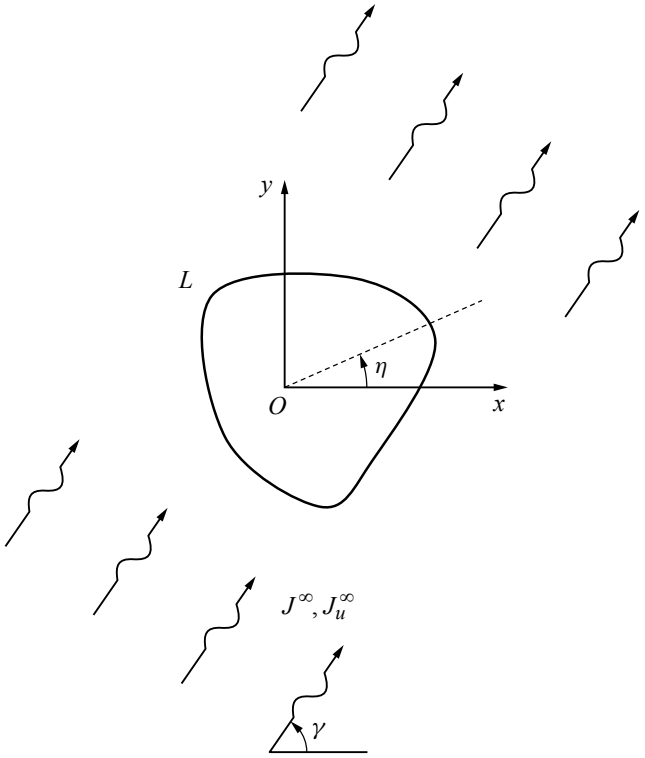

Figure 1. An infinite thermoelectric medium containing an arbitrarily-shaped hole.

the associated thermal stress field is obtainable from determining the complex functions $\varphi(z)$ and $\psi(z)$ based on the known temperature field and the stress boundary conditions described as the last in (18).

3.2. ***Series representations.*** Before embarking on the problem, we first introduce a conformal mapping of a truncated form, which associates the infinite region outside the hole in the z-plane with the exterior of the unit circle in the imaginary ξ-plane (see Figure 2), as [Dai et al. 2014]

$$z = \omega(\xi) = R\left(\xi + \sum_{j=1}^{M} m_j \xi^{-j}\right) e^{i\eta}, \quad |\xi| \geq 1, \tag{19}$$

where M is a positive integer, the parameter R, m_j $(j = 1, 2, \ldots, M)$ and η controls the overall size, shape and rotation of the hole. It should be mentioned that although (19) does not accomplish the mapping of an arbitrarily shaped hole, it can be made to approximate as closely as desired the shape of a wide variety of boundaries by the simple expedient of increasing the degree of the polynomial [Muskhelishvili 1975; Dai et al. 2014].

According to the single-value conditions of the thermoelectric potential (see (7)) and the equilibrium of the normal electric current density on the entire boundary (see the first in (12)), it is concluded that the derivative of the potential function $f'(z)$ must be single-valued, but $f(z)$ itself may be multi-valued. In the context of the mapping (19), one can give the expression of the thermoelectric potential function $f(z)$

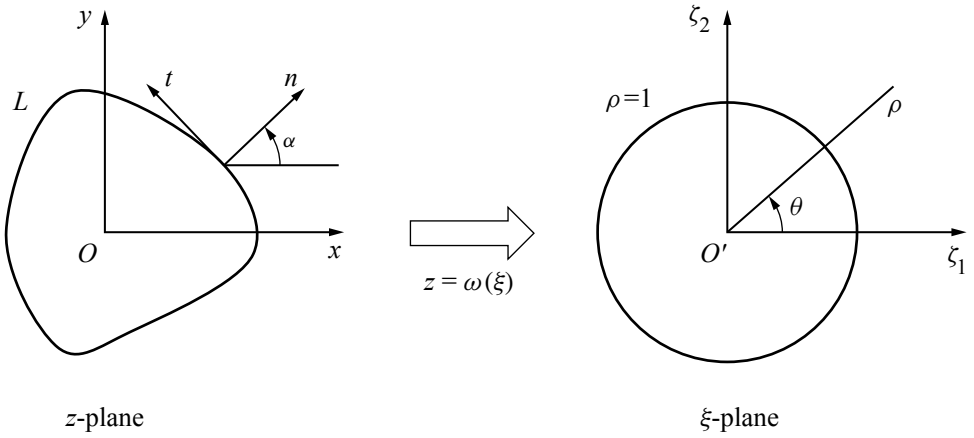

Figure 2. Conformal mapping.

via a truncated form as

$$f(z) = \frac{\Gamma_1}{2} z^2 + A \ln \xi + \sum_{j=1}^{N-1} a_j \xi^{-1}, \tag{20}$$

where Γ_1 is a complex constant to be determined from the remote electric current density. Inserting (20) into (8) and taking the limit $z \to \infty$ leads to

$$\Gamma_1 = -\frac{J^\infty e^{-i\gamma}}{\delta}. \tag{21}$$

A and a_j $(j = 1, 2, \ldots, N-1)$ are unknown complex coefficients to be determined. The chain rule gives

$$\frac{d}{dz} = \frac{d}{d\xi} \cdot \frac{d\xi}{dz} = \frac{1}{\omega'(\xi)} \cdot \frac{d}{d\xi}, \tag{22}$$

so the first and second spatial derivatives of $f(z)$ are

$$f'(z) = \Gamma_1 z + \frac{1}{\omega'(\xi)} \left(A\xi^{-1} - \sum_{j=1}^{N-1} j a_j \xi^{-j-1} \right), \tag{23}$$

$$f''(z) = \Gamma_1 + \frac{\left(-A\xi^{-2} + \sum_{j=1}^{N-1} j(j+1) a_j \xi^{-j-2}\right) \omega'(\xi) - \left(A\xi^{-1} - \sum_{j=1}^{N-1} j a_j \xi^{-j-1}\right) \omega''(\xi)}{\omega'(\xi)^3}. \tag{24}$$

The electrically insulated boundary condition on L can be expressed, according to (12), as

$$f'(z) = \overline{f'(z)}, \quad z \in L. \tag{25}$$

By using (23), boundary condition (25) can be rewritten as

$$\Gamma_1 \omega(\sigma) + \frac{1}{\omega'(\sigma)} \left(A\sigma^{-1} - \sum_{j=1}^{N-1} j a_j \sigma^{-j-1} \right) = \overline{\Gamma}_1 \overline{\omega(\sigma)} + \frac{1}{\overline{\omega'(\sigma)}} \left(\overline{A}\sigma - \sum_{j=1}^{n-1} j \overline{a_j} \sigma^{j+1} \right). \tag{26}$$

Then we expand every part of (26) into truncated Fourier series along boundary L:

$$\begin{aligned}
\frac{\sigma^{-1}}{\omega'(\sigma)} &= \sum_{k=-N}^{N} b_k^{(1)}\sigma^k, \qquad b_k^{(1)} = \frac{1}{2\pi}\int_0^{2\pi} \frac{\sigma^{-1}}{\omega'(\sigma)}\cdot\sigma^{-k}\,d\theta,\\
\frac{\sigma}{\overline{\omega'(\sigma)}} &= \sum_{k=-N}^{N} b_k^{(2)}\sigma^k, \qquad b_k^{(2)} = \frac{1}{2\pi}\int_0^{2\pi} \frac{\sigma}{\overline{\omega'(\sigma)}}\cdot\sigma^{-k}\,d\theta,\\
\frac{-j\sigma^{-j-1}}{\omega'(\sigma)} &= \sum_{k=-N}^{N} b_{j,k}^{(3)}\sigma^k, \qquad b_{j,k}^{(3)} = \frac{1}{2\pi}\int_0^{2\pi} \frac{-j\sigma^{-j-1}}{\omega'(\sigma)}\cdot\sigma^{-k}\,d\theta,\\
\frac{-j\sigma^{j+1}}{\omega'(\sigma)} &= \sum_{k=-N}^{N} b_{j,k}^{(4)}\sigma^k, \qquad b_{j,k}^{(4)} = \frac{1}{2\pi}\int_0^{2\pi} \frac{-j\sigma^{j+1}}{\overline{\omega'(\sigma)}}\cdot\sigma^{-k}\,d\theta,
\end{aligned} \tag{27}$$

where $b_k^{(1)}$ and $b_k^{(2)}$ are coefficients independent of j, while $b_{j,k}^{(3)}$ and $b_{j,k}^{(4)}$ are those related to j. These coefficients can be calculated numerically by Gaussian quadrature. Hence, (26) can be rewritten as

$$\Gamma_1\omega(\sigma) + A\sum_{k=-N}^{N} b_k^{(1)}\sigma^k + \sum_{k=-N}^{N}\sum_{j=1}^{n-1} a_j b_{j,k}^{(3)}\sigma^k = \overline{\Gamma_1}\,\overline{\omega(\sigma)} + \bar{A}\sum_{k=-N}^{N} b_k^{(2)}\sigma^k + \sum_{k=-N}^{N}\sum_{j=1}^{N-1}\overline{a_j}\, b_{j,k}^{(4)}\sigma^k. \tag{28}$$

Equating the coefficients of σ^j, $j = 1, 2, \ldots, N$, yields N complex equations which are equivalent to $2N$ real equations. Clearly, these real equations are linear with respect to the real and imaginary parts of all the complex coefficients A and a_j $(j = 1, 2, \ldots, N-1)$. Once all the complex coefficients are determined by solving these linear equations, the thermoelectric potential $f(z)$ can be easily obtained through (20).

In the same manner, the potential functions $g(z)$ and its derivative should take the following forms:

$$g(z) = \frac{\Gamma_3}{3}z^3 + \frac{\Gamma_2}{2}z^2 + C\ln\xi + \sum_{j=1}^{2N-1} c_j\xi^{-1}, \tag{29}$$

$$g'(z) = \Gamma_3 z^2 + \Gamma_2 z + \frac{1}{\omega'(\xi)}\left(C\xi^{-1} - \sum_{j=1}^{2N-1} j c_j\xi^{-j-1}\right), \tag{30}$$

where Γ_2 and Γ_3 are two complex constants to be determined from the remote energy flux condition. Inserting (20) and (30) into (11) and taking the limit $z \to \infty$ gives

$$\Gamma_2 = -\frac{J_u^{\infty} e^{-i\gamma}}{\kappa}, \qquad \Gamma_3 = -\frac{\delta}{4\kappa}\Gamma_1^2 = -\frac{J^{\infty 2} e^{-2i\gamma}}{4\kappa\delta}. \tag{31}$$

The remaining constant coefficients C and c_j, $(j = 1, 2, \ldots, 2N-1)$ may be determined from the thermal boundary condition on the hole rim. According to (13) and the second of (18), the thermally insulated boundary condition on the hole rim L is expressed by

$$g'(z) + \frac{\delta}{4\kappa}f'(z)^2 = \overline{g'(z)} + \frac{\delta}{4\kappa}\,\overline{f'(z)}^2, \quad z \in L. \tag{32}$$

From (30), one has

$$\Gamma_3\omega(\sigma)^2+\Gamma_2\omega(\sigma)+\frac{1}{\omega'(\sigma)}\left(C\sigma^{-1}-\sum_{j=1}^{2N-1}jc_j\sigma^{-j-1}\right)+\frac{\delta}{4\kappa}f'^2(\sigma)$$
$$=\overline{\Gamma_3}\,\overline{\omega(\sigma)}^2+\overline{\Gamma_2}\,\overline{\omega(\sigma)}+\frac{1}{\overline{\omega'(\sigma)}}\left(\bar{C}\sigma-\sum_{j=1}^{2N-1}j\,\overline{c_j}\,\sigma^{j+1}\right)+\frac{\delta}{4\kappa}\,\overline{f'^2(\sigma)}, \quad (33)$$

where $f'(\sigma)$ represents the boundary value of function $f'(z)$ on the boundary $z=\omega(\sigma)\in L$. Note that the thermoelectric potential $f'(z)$ is determined in the above section as

$$\begin{aligned} f'(\sigma)&=f'[\omega(\sigma)]=\Gamma_1\omega(\sigma)+A\sum_{k=-N}^{N}b_k^{(1)}\sigma^k+\sum_{k=-N}^{N}\sum_{j=1}^{N-1}a_j\,b_{j,k}^{(3)}\sigma^k,\\ \overline{f'(\sigma)}&=\overline{f'[\omega(\sigma)]}=\overline{\Gamma_1}\,\overline{\omega(\sigma)}+\bar{A}\sum_{k=-N}^{N}b_k^{(2)}\sigma^k+\sum_{k=-N}^{N}\sum_{j=1}^{N-1}\overline{a_j}\,b_{j,k}^{(4)}\sigma^k. \end{aligned} \quad (34)$$

In what follows, the Fourier series method is also taken to deal with the boundary condition (33) as what we did on (26). Here we expand both sides of (33) into the Fourier series of σ by numerical quadrature, respectively, and then equate the coefficients of σ^j $(j=1,2,\ldots,2N)$ on the two sides of (33), leading to $2N$ complex equations (equivalent to $4N$ real equations) which are linear with respect to the real and imaginary parts of all the complex coefficients C and c_j $(j=1,2,\ldots,2N-1)$. Finally, all the unknowns are obtained through solving the linear system of equations.

Since no far-field mechanical loads are imposed on the medium and only the electrically and thermally induced stresses are considered here, the two elastic potentials $\varphi(z)$ and $\psi(z)$ can be expressed in terms of truncated series as

$$\varphi(z)=P(\xi)\ln\xi+\sum_{j=1}^{2N}p_j\,\xi^{-1},\qquad \psi(z)=Q(\xi)\ln\xi+\sum_{j=1}^{2N}q_j\,\xi^{-1}, \quad (35)$$

where p_j and q_j are complex coefficients to be determined, and the coefficients $P(\xi)$ and $Q(\xi)$ identifying the multi-valued terms can be specified, according to the single-value condition of displacement (see (16)) and the vanishing resultant force vector over the entire boundary L (see (17)), as

$$P(\xi)=P_0=-\frac{2\mu\lambda C}{\beta+1},\qquad Q(\xi)=\overline{P_0}+\frac{k\delta\bar{A}}{8\kappa}f'(\xi), \quad (36)$$

where $f'(\xi)=f'[\omega(\xi)]$. According to (17), the traction-free condition on the hole surface (the last in (18)) can be expressed by

$$P_0\ln\sigma+\sum_{j=1}^{2N}p_j\,\sigma^{-1}+\frac{\omega(\sigma)}{\overline{\omega'(\sigma)}}\left(\overline{P_0}\,\sigma-\sum_{j=1}^{2N}\overline{P_j}\,j\sigma^{j+1}\right)$$
$$-\left[P_0+\frac{k\delta A}{8\kappa}\,\overline{f'(\sigma)}\right]\ln\sigma+\sum_{j=1}^{2N}\overline{q_j}\,\sigma^j+\frac{k\delta}{8\kappa}\,\overline{f'(\sigma)}\,f(\sigma)=0, \quad (37)$$

where

$$f(\sigma) = f[\omega(\sigma)] = \frac{\Gamma_1}{2}\omega(\sigma)^2 + A\ln\sigma + \sum_{j=1}^{N} a_j \sigma^{-j}. \tag{38}$$

In the same manner, the Fourier series method is also taken to deal with the boundary condition (37). As what we did on (26), here we expand both sides of (37) into the Fourier series of σ by numerical quadrature, respectively, and then equate the coefficients of σ^j $(-2N, -2N+1, \ldots, -1, 1, 2, \ldots, 2N)$ on the two sides of (37), leading to $4N$ complex equations which can be used to determine all the complex coefficients p_j and q_j $(j = 1, 2, \ldots, 2N)$. Once all the complex coefficients are obtained, the complex potentials $\varphi(z)$ and $\psi(z)$ can be determined by noting (35) and (36), and therefore the stress fields in the material are obtained. Using the stress transformation formula, stress components in the material in polar coordinates can be determined by

$$\sigma_{nm} + \sigma_{tt} = \sigma_{yy} + \sigma_{xx}, \qquad \sigma_{tt} - \sigma_{nm} + 2i\sigma_{nt} = e^{2i\alpha}(\sigma_{yy} - \sigma_{xx} + 2i\sigma_{xy}), \tag{39}$$

where σ_{nn}, σ_{tt} and σ_{nt} are the normal stress, hoop stress and shear stress, respectively, and α is the angle between the outer normal on L and the positive x-axis in the z-plane, which is determined by

$$e^{2i\alpha} = \frac{\xi^2 \omega'(\xi)}{\rho^2 \overline{\omega'(\xi)}}. \tag{40}$$

4. Numerical examples

So far, the analytical solutions for the problem of an arbitrarily-shaped hole have been obtained in the form of a finite series. To verify the compatibility and the feasibility of our proposed solutions, we present some examples and compare the results obtained from the presented method with those of the previous work. Firstly, an electrically and thermally insulated elliptical hole in a thermoelectric medium under different loading conditions is considered. The mapping function for the elliptical hole is given by

$$z = \omega(\xi) = R\left(\xi + \frac{m}{\xi}\right), \tag{41}$$

where $R = (a+b)/2$ and $m = (a-b)/(a+b)$ with a and b being the semi-major and the semi-minor axes of the elliptical hole. In the case of $a/b = 5$, the hoop stress distributions around the elliptical hole when only the remote electric current load is imposed and only the remote energy flux load is applied along the positive y-axis are plotted in Figure 3 (top left) and Figure 3 (top right), respectively. It should be mentioned that the stresses produced by the applied electric current and energy flux loads in thermoelectric materials are found to be uncoupled according to [Wang and Wang 2017], which enables us to analyze the effects of the electric current and energy flux loads separately. Furthermore, $\sigma_{e0} = kJ^{\infty 2}R^2/8\delta\kappa$ and $\sigma_{u0} = 2\mu\lambda J_u^{\infty} R/\kappa(\beta+1)$, which have the same unit as stresses, are used to normalize the hoop stresses caused by the far-field electric current and energy flux loads, respectively. It is clearly seen that the results obtained by our solution agree very well with those given by Wang and Wang [2017] for an insulated elliptical hole.

To further verify the compatibility of the presented solutions, we consider the generalized thermoelastic problems of a thermally insulated quasi-square hole and a thermally insulated ovaloid hole in

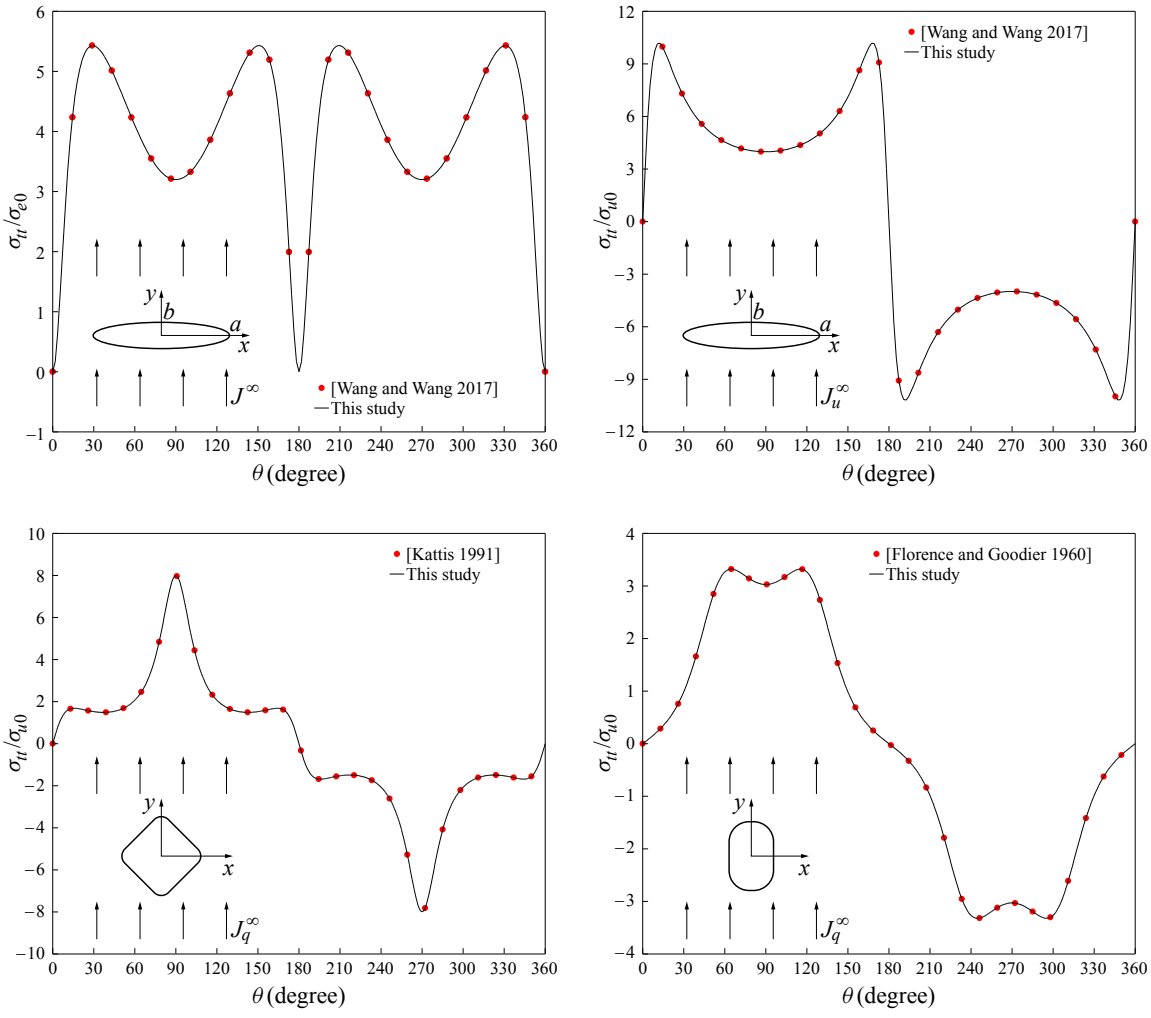

Figure 3. Comparisons of the present work to the previous work for some special cases.

an infinite elastic matrix subjected to a uniform thermal flux. To this end, the medium in this case is considered to be electrically insulated, that is, $\delta = 0$. Thus, no electric current exists in the material and the energy flux is completely equivalent to the heat flux, as seen from (1) and (4). The mapping functions (19) for the quasi-square hole and the oval hole considered here are given by

$$\begin{aligned} z = \omega(\xi) &= R\left(\xi + \frac{1}{8}\xi^{-3}\right), && \text{(Square hole)},\\ z = \omega(\xi) &= R\left(\xi - \frac{1}{5}\xi^{-1} - \frac{1}{20}\xi^{-3}\right), && \text{(Ovaloid hole)}. \end{aligned} \tag{42}$$

A comparison between the results of the present study and the results obtained by Kattis [1991] for a square hole is plotted in Figure 3 (bottom left). Here, $\sigma_{q0} = 2\mu\lambda J_q^{\infty} R/\kappa(\beta+1)$ is used to normalize

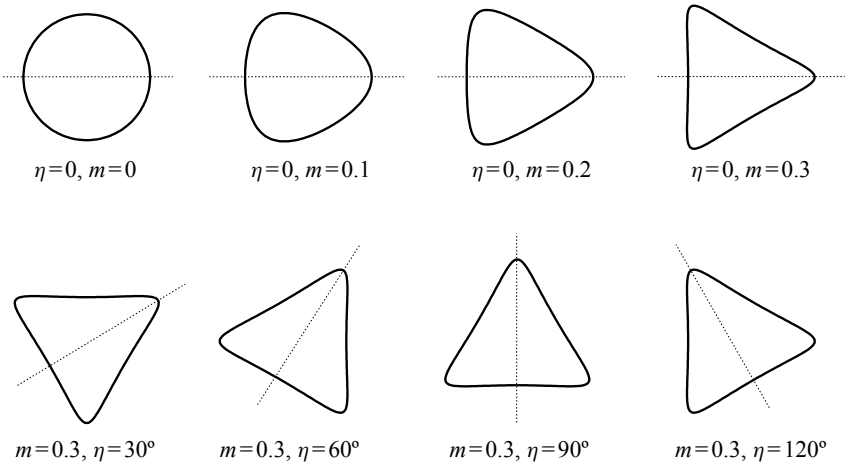

Figure 4. The effect of parameters m and η on the hole shape.

the hoop stresses produced by the far-field thermal flux. In addition, Figure 3 (bottom right) shows the comparison of our solution with that of Florence and Goodier [1960] for the ovaloid cutout under a uniform thermal flux applied at infinity. It can be found that the normalized hoop stress around the holes of given shapes obtained by the presented solution are almost identical to those of the previous work, which further verifies the validity of the present formulation.

To illustrate the application of the analysis method, the hoop stress around a triangular hole will be presented below. For the triangular hole, the mapping function (19) can be given as

$$z = \omega(\xi) = R(\xi + m\xi^{-2})\, e^{i\eta}. \tag{43}$$

The conditions $0 \le m < 1/2$ ensure that the hole shape does not have loops. The radius of curvature at the corner of the hole and the orientation of the hole vary by changing the parameters m and η, respectively, as shown in Figure 4. It can be seen that the corner of the hole becomes sharper with increasing the parameter m.

The distribution of the electric current on the hole rim when a uniform electric current is solely loaded along the positive y-axis is plotted in Figure 5. It is found that the electric current around the triangular hole has a concentration at the corners. As the corner becomes sharper, the electric current concentration is more obvious. For given load direction ($\gamma = 90°$) and hole orientation ($\eta = 0$), the maximum concentration of the electric current on the hole occurs at $\theta = 0$. Furthermore, the distributions of energy flux under a uniform energy load is found to be similar with that of the electric current and thus a similar conclusion could be drawn.

When there is only electric current loaded along the vertical direction ($\gamma = 90°$), the distribution of the normalized hoop stress around the hole is plotted in Figure 6. Likely, when there is only energy flux imposed along the vertical direction, the distribution of the normalized hoop stress is plotted in Figure 7. Here, the hole orientation is set to be zero, namely $\eta = 0$. We find that both applied electric current and energy flux generate thermal stress around hole and thermal stress becomes more concentrated as the corner becomes sharper. In addition, the maximum stress concentration generated by both electric

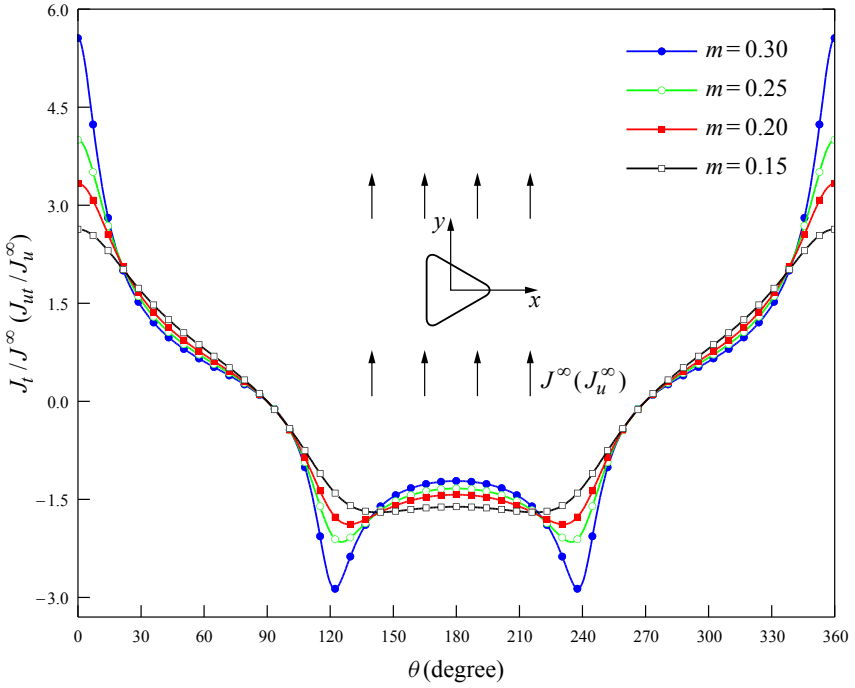

Figure 5. Variation of normalized electric current (energy flux) on the hole rim with θ when $J^\infty(J_u^\infty)$ is solely applied.

current and energy flux occurs at $\theta = 120°$ and $\theta = 240°$ in this case. The difference is that the applied electric current produces thermal stress concentration at the corner of $\theta = 0°$ but the energy flux load does not under the same loading condition. Another difference is that the applied energy flux produces the opposite stress state on any two points symmetric with respect to x-axis, however, the imposed electric current produces the same stress state.

Figures 8 and 9 show the periodic behavior of the remote electric current and energy flux induced hoop stress at point $\theta = 0°$ in terms of load angle γ, respectively. These results have been presented for the case of $\eta = 0$. It can be seen from Figure 8 that hoop stress induced by J^∞ varies periodically as the load angle γ changes (with a period of 180°). According to Figure 9, the stress induced by J_u^∞ is also a periodic function of the load angle γ, however, the period becomes to be 360°. When $\gamma = 90°$ or 270°, both the electric current and energy flux induced hoop stresses reach their minimum values.

The interesting results shown in Figures 10 and 11 are that for given load angle $\gamma = 90°$, the maximum hoop stress induced by J^∞ and J_u^∞ varies when the rotation of the hole η is changed. The normalized hoop stress produced by J^∞ obtained its maximum value when the hole oriented at 30° and 90°. On the other hand, the normalized hoop stress produced by J_u^∞ obtained its maximum value when $\eta = 30°$ and obtained its minimum value when $\eta = 90°$. It should be mentioned that the maximum normalized stresses are very important in design and implementation for thermoelectric devices. The maximum normalized stress might cause damages to thermoelectric structure and thus should be avoided.

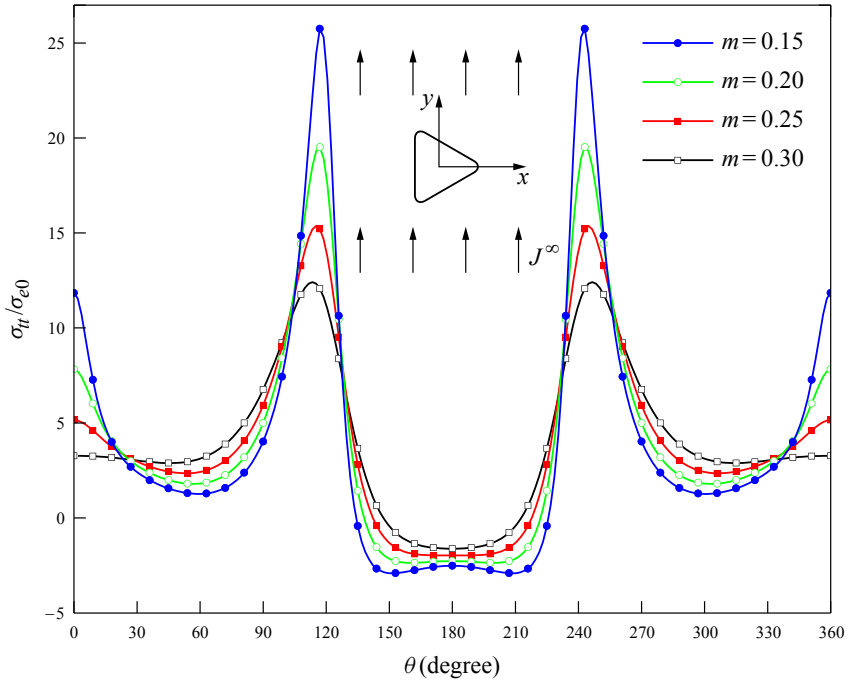

Figure 6. Variation of normalized hoop stress with θ when J^{∞} is solely applied.

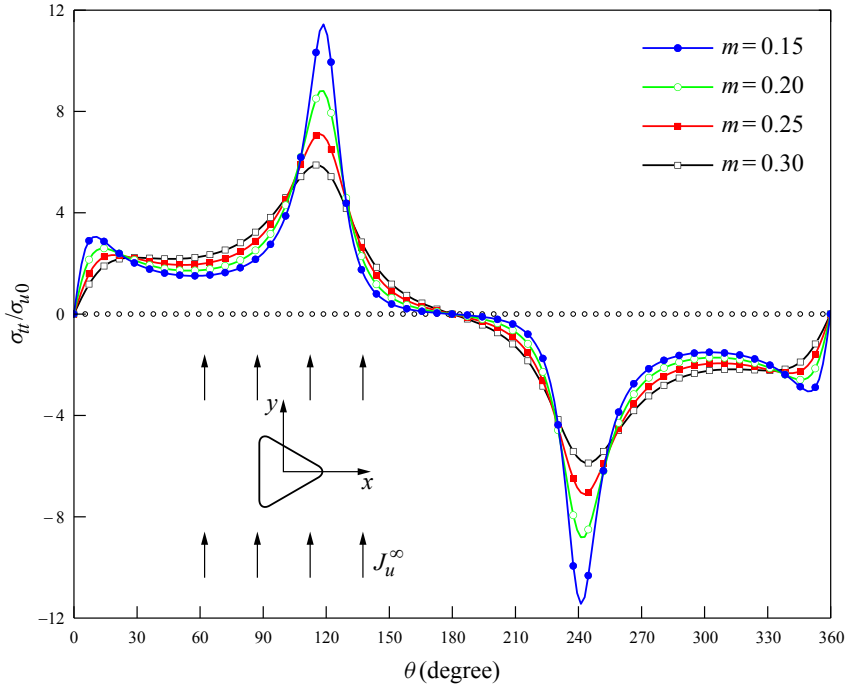

Figure 7. Variation of normalized hoop stress with θ when J_u^{∞} is solely applied.

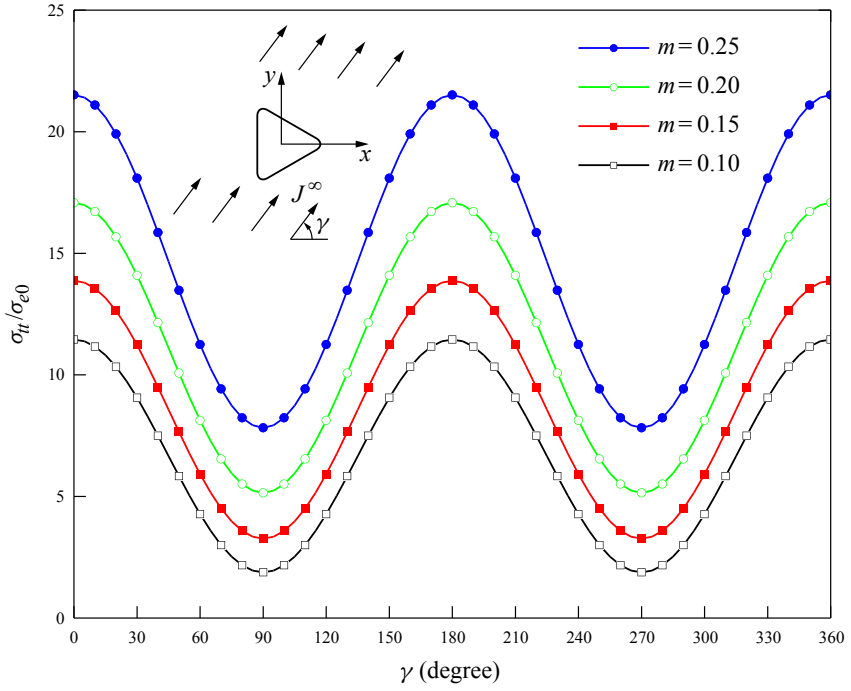

Figure 8. Periodic behavior of hoop stress at $\theta = 0°$ in terms of γ when J^{∞} is solely applied.

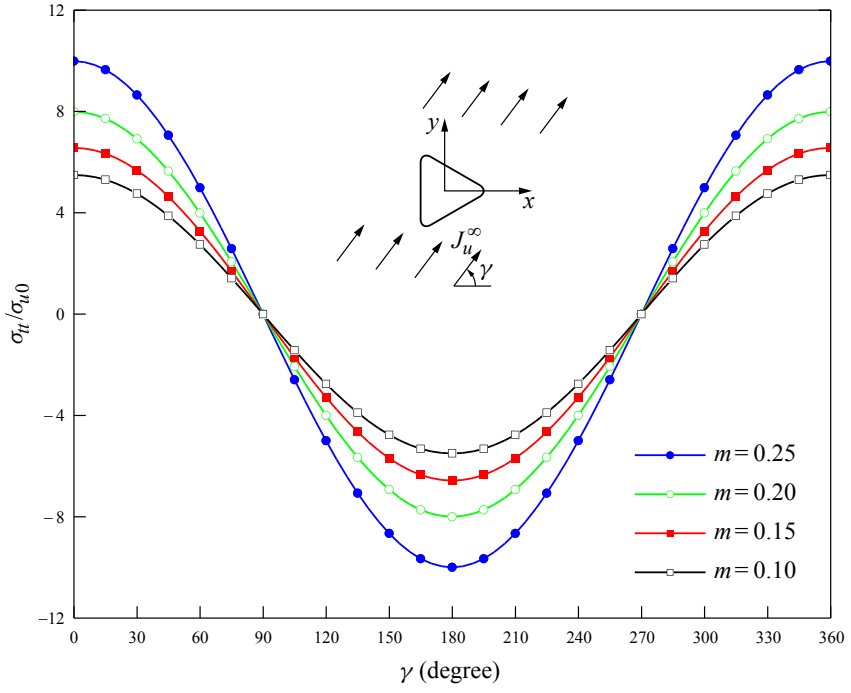

Figure 9. Periodic behavior of hoop stress at $\theta = 0°$ in terms of γ when J_u^{∞} is solely applied.

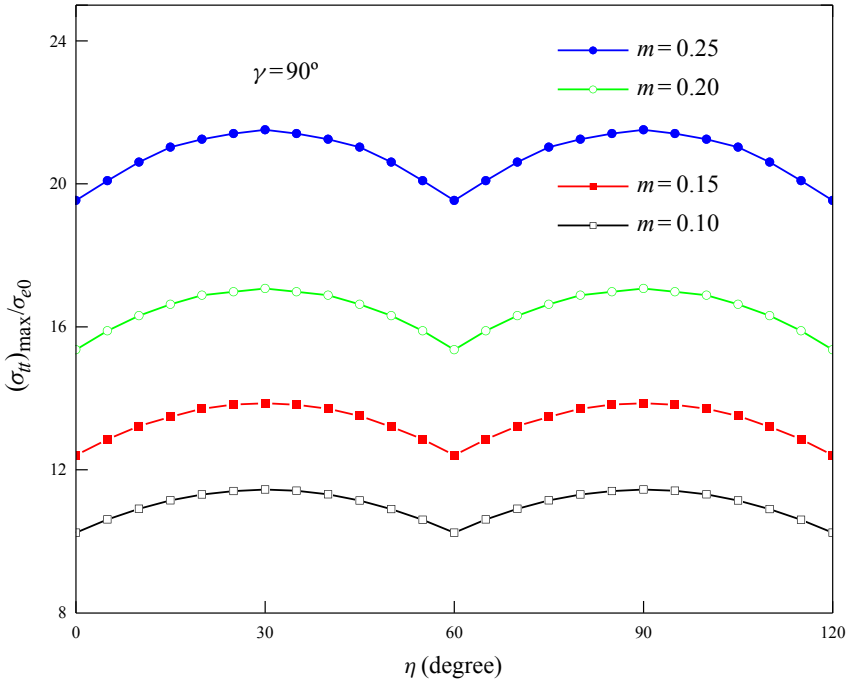

Figure 10. Variation of the maximum normalized hoop stress with η when J^{∞} is solely applied.

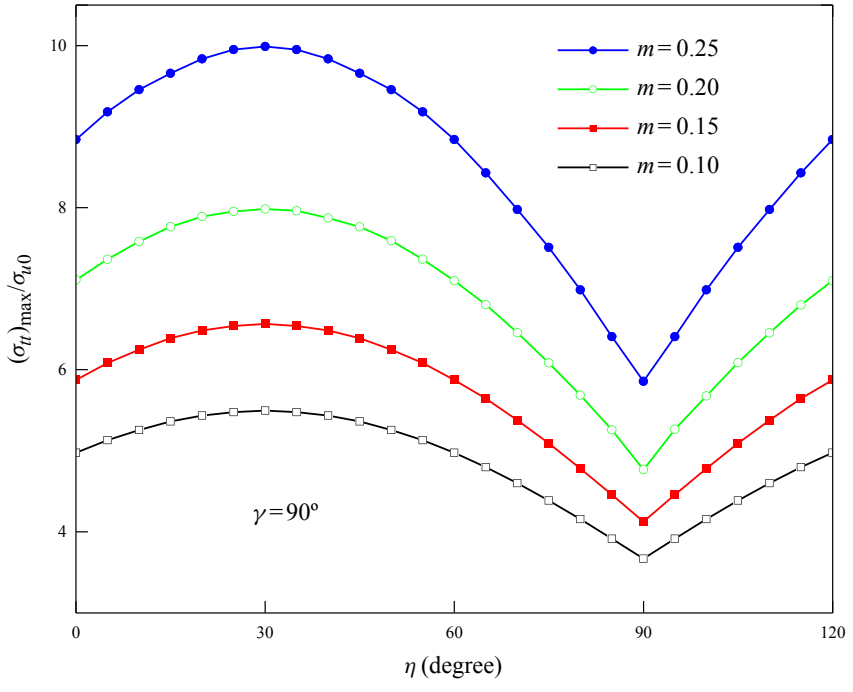

Figure 11. Variation of the maximum normalized hoop stress with η when J_u^{∞} is solely applied.

5. Concluding remarks

Stress concentration around the holes is of practical importance in designing of the thermoelectric structures. The hole shape is one of the important parameters that affects the location and amount of maximum hoop stress. Based on the complex variable method, a simple analytical solution was presented in this study. This solution provided a numerical result to obtain the normalized hoop stress for thermoelectric materials with regular holes with various shapes. Numerical study was conducted to investigate the effects of different parameters such as the load angle, rotation angle of hole, bluntness on the hoop stress. The results show that the loading angle and hole orientation have a significant impact in reducing the normalized stress in addition to increasing the bluntness. By the correct selection of these parameters, the lowest amount of thermal stress could be achieved.

Acknowledgements

Yu and Gao acknowledge the support from the National Natural Science Foundation of China (Grant Number 11232007 and 11472130) and a Project Funded by the Priority Academic Program Development of Jiangsu Higher Education Institutions (PAPD). Yang thanks the support from the National Natural Science Foundation of China (Grant Number 11702147).

References

[Bell 2008] L. E. Bell, "Cooling, heating, generating power, and recovering waste heat with thermoelectric systems", *Science* **321**:5895 (2008), 1457–1461.

[Chao and Wang 1993] C. K. Chao and J. L. Wang, "Failure prediction of a plate weakened by an elliptic hole under thermal or mechanical load", *Eng. Fract. Mech.* **45**:6 (1993), 843–856.

[Chen and Chao 2008] F. M. Chen and C. K. Chao, "Stress analysis of an infinite plate with a coated elliptic hole under a remote uniform heat flow", *J. Therm. Stresses* **31**:7 (2008), 599–613.

[Dai et al. 2014] M. Dai, C.-F. Gao, and C. Q. Ru, "Surface tension-induced stress concentration around a nanosized hole of arbitrary shape in an elastic half-plane", *Meccanica* (*Milano*) **49**:12 (2014), 2847–2859.

[Florence and Goodier 1960] A. L. Florence and J. N. Goodier, "Thermal stresses due to disturbance of uniform heat flow by an insulated ovaloid hole", *J. Appl. Mech.* (*ASME*) **27**:4 (1960), 635–639.

[Gao et al. 2002] C.-F. Gao, Y.-T. Zhao, and M.-Z. Wang, "An exact and explicit treatment of an elliptic hole problem in thermopiezoelectric media", *Int. J. Solids Struct.* **39**:9 (2002), 2665–2685.

[Hasebe 2009] N. Hasebe, "Magneto-elastic stress induced by an electric current in an infinite thin plate with an elliptical hole", *Arch. Appl. Mech.* **80**:12 (2009), 1353–1370.

[Hasebe and Wang 2005] N. Hasebe and X. Wang, "Complex variable method for thermal stress problem", *J. Therm. Stresses* **28**:6-7 (2005), 595–648.

[Hasebe et al. 2009] N. Hasebe, C. Bucher, and R. Heuer, "Analyses of thermal conduction and stress induced by electric current in an infinite thin plate with an elliptical hole", *J. Therm. Stresses* **32**:10 (2009), 1065–1086.

[He and Tritt 2017] J. He and T. M. Tritt, "Advances in thermoelectric materials research: looking back and moving forward", *Science* **357**:6358 (2017), eaak9997.

[He et al. 2015] W. He, G. Zhang, X. Zhang, J. Ji, G. Li, and X. Zhao, "Recent development and application of thermoelectric generator and cooler", *Appl. Energy* **143**:1 (2015), 1–25.

[Jafari et al. 2016] M. Jafari, M. B. Nazari, and A. Taherinasab, "Thermal stress analysis in metallic plates with a non-circular hole subjected to uniform heat flux", *Eur. J. Mech. A Solids* **59** (2016), 356–363.

[Kattis 1991] M. A. Kattis, "Thermoelastic plane problems with curvilinear boundaries", *Acta Mech.* **87**:1-2 (1991), 93–103.

[Li et al. 2015] G. Li, Q. An, W. Li, W. A. Goddard, P. Zhai, Q. Zhang, and G. J. Snyder, "Brittle failure mechanism in thermoelectric skutterudite $CoSb_3$", *Chem. Mater.* **27**:18 (2015), 6329–6336.

[Muskhelishvili 1975] N. I. Muskhelishvili, *Some basic problems of the mathematical theory of elasticity*, Noordhoff, Groningen, 1975.

[Pang et al. 2018] S.-J. Pang, Y.-T. Zhou, and F.-J. Li, "Analytic solutions of thermoelectric materials containing a circular hole with a straight crack", *Int. J. Mech. Sci.* **144** (2018), 731–738.

[Qin 1999] Q.-H. Qin, "Green's function for thermopiezoelectric plates with holes of various shapes", *Arch. Appl. Mech.* **69**:6 (1999), 406–418.

[Qin 2000] Q.-H. Qin, "General solutions for thermopiezoelectrics with various holes under thermal loading", *Int. J. Solids Struct.* **37**:39 (2000), 5561–5578.

[Rasouli and Jafari 2016] M. Rasouli and M. Jafari, "Thermal stress analysis of infinite anisotropic plate with elliptical hole under uniform heat flux", *J. Therm. Stresses* **39**:11 (2016), 1341–1355.

[Schmidt et al. 2015] R. D. Schmidt, X. Fan, E. D. Case, and P. B. Sarac, "Mechanical properties of Mg_2Si thermoelectric materials with the addition of 0–4 vol% silicon carbide nanoparticles (SiC_{NP})", *J. Mater. Sci.* **50**:11 (2015), 4034–4046.

[Tritt and Subramanian 2006] T. M. Tritt and M. A. Subramanian, "Thermoelectric materials, phenomena, and applications: a bird's eye view", *MRS Bull.* **31**:3 (2006), 188–198.

[Wang and Wang 2017] P. Wang and B. L. Wang, "Thermoelectric fields and associated thermal stresses for an inclined elliptic hole in thermoelectric materials", *Int. J. Eng. Sci.* **119** (2017), 93–108.

[Yang and Gao 2010] Q. Yang and C.-F. Gao, "Non-axisymmetric thermal stress around a circular hole in a functionally graded infinite plate", *J. Therm. Stresses* **33**:4 (2010), 318–334.

[Yang et al. 2013] Y. Yang, F. Y. Ma, C. H. Lei, Y. Y. Liu, and J. Y. Li, "Nonlinear asymptotic homogenization and the effective behavior of layered thermoelectric composites", *J. Mech. Phys. Solids* **61**:8 (2013), 1768–1783.

[Yoshikawa and Hasebe 1999] K. Yoshikawa and N. Hasebe, "Green's function for a heat source in an infinite region with an arbitrary shaped hole", *J. Appl. Mech.* (*ASME*) **66**:1 (1999), 204–210.

[Yu et al. 2017] C. Yu, D. Zou, Y.-H. Li, H.-B. Yang, and C.-F. Gao, "An arc-shaped crack in nonlinear fully coupled thermoelectric materials", *Acta Mech.* **229**:5 (2017), 1989–2008.

[Zhang and Wang 2016] A. B. Zhang and B. L. Wang, "Explicit solutions of an elliptic hole or a crack problem in thermoelectric materials", *Eng. Fract. Mech.* **151** (2016), 11–21.

Received 20 Sep 2018. Revised 24 Mar 2019. Accepted 29 May 2019.

CHUAN-BIN YU: cbyu@nuaa.edu.cn
State Key Laboratory of Mechanics and Control of Mechanical Structures, Nanjing University of Aeronautics and Astronautics, Nanjing, 210016, China

HAI-BING YANG: yanghb@scut.edu.cn
Department of Mechanics Engineering, School of Civil Engineering and Transportation, South China University of Technology, Guangzhou, 510641, China

KUN SONG: ksong3@ualberta.ca
State Key Laboratory of Mechanics and Control of Mechanical Structures, Nanjing University of Aeronautics and Astronautics, Nanjing, 210016, China

CUN-FA GAO: cfgao@nuaa.edu.cn
State Key Laboratory of Mechanics and Control of Mechanical Structures, Nanjing University of Aeronautics and Astronautics, Nanjing, 210016, China

JOURNAL OF MECHANICS OF MATERIALS AND STRUCTURES

msp.org/jomms

Founded by Charles R. Steele and Marie-Louise Steele

EDITORIAL BOARD

ADAIR R. AGUIAR	University of São Paulo at São Carlos, Brazil
KATIA BERTOLDI	Harvard University, USA
DAVIDE BIGONI	University of Trento, Italy
MAENGHYO CHO	Seoul National University, Korea
HUILING DUAN	Beijing University
YIBIN FU	Keele University, UK
IWONA JASIUK	University of Illinois at Urbana-Champaign, USA
DENNIS KOCHMANN	ETH Zurich
MITSUTOSHI KURODA	Yamagata University, Japan
CHEE W. LIM	City University of Hong Kong
ZISHUN LIU	Xi'an Jiaotong University, China
THOMAS J. PENCE	Michigan State University, USA
GIANNI ROYER-CARFAGNI	Università degli studi di Parma, Italy
DAVID STEIGMANN	University of California at Berkeley, USA
PAUL STEINMANN	Friedrich-Alexander-Universität Erlangen-Nürnberg, Germany
KENJIRO TERADA	Tohoku University, Japan

ADVISORY BOARD

J. P. CARTER	University of Sydney, Australia
D. H. HODGES	Georgia Institute of Technology, USA
J. HUTCHINSON	Harvard University, USA
D. PAMPLONA	Universidade Católica do Rio de Janeiro, Brazil
M. B. RUBIN	Technion, Haifa, Israel

PRODUCTION production@msp.org

SILVIO LEVY Scientific Editor

Cover photo: Mando Gomez, www.mandolux.com

See msp.org/jomms for submission guidelines.

JoMMS (ISSN 1559-3959) at Mathematical Sciences Publishers, 798 Evans Hall #6840, c/o University of California, Berkeley, CA 94720-3840, is published in 10 issues a year. The subscription price for 2019 is US $635/year for the electronic version, and $795/year (+$60, if shipping outside the US) for print and electronic. Subscriptions, requests for back issues, and changes of address should be sent to MSP.

JoMMS peer-review and production is managed by EditFLOW® from Mathematical Sciences Publishers.

PUBLISHED BY

mathematical sciences publishers

nonprofit scientific publishing

http://msp.org/

© 2019 Mathematical Sciences Publishers

Journal of Mechanics of Materials and Structures

Volume 14, No. 2 March 2019

A mode-dependent energy-based damage model for peridynamics and its implementation
CHRISTIAN WILLBERG, LASSE WIEDEMANN and MARTIN RÄDEL 193

Elastic wave propagation in a periodic composite plate structure: band gaps incorporating microstructure, surface energy and foundation effects
GONGYE ZHANG and XIN-LIN GAO 219

Dynamic analysis of a mass traveling on a simply supported nonhomogeneous beam composed of transversely embedded periodic arrays
YI-MING WANG and HUNG-CHIEH LIU 237

Stress concentration around an arbitrarily-shaped hole in nonlinear fully coupled thermoelectric materials
CHUAN-BIN YU, HAI-BING YANG, KUN SONG and CUN-FA GAO 259

The effect of variable thermal conductivity on an infinite fiber-reinforced thick plate under initial stress
MOHAMED I. A. OTHMAN, AHMED E. ABOUELREGAL and SAMIA M. SAID 277

Large deflections and stability of spring-hinged cantilever beam MILAN BATISTA 295

1559-3959(2019)14:2;1-W